DOI: 10.5185/amlett.2025.021775

OPEN ACCESS

RESEARCH

Research on Electrical Characteristics of Composite Biological Tissue Junction Based on Active Electric Field Principle

Cong Yang¹, Tian Tian², Long Wang¹, Dehao Yin¹, Jiegang Peng¹*

¹School of Automation Engineering, University of Electronic Science and Technology of China, Xiyuan Avenue 2006, High tech Zone, Chengdu, 610000, China

²Department of Obstetrics and Gynecology Sichuan Provincial People's Hospital, University of Electronic Science and Technology of China, No. 32, West Section 2, First Ring Road, Qingyang District, Chengdu, 610072, China

*Corresponding author: E-mail: pjg2000cn@hotmail.com

ABSTRACT

This study aims to explore the unique electrical properties of organic tissue junctions with different electrical properties in an active electric field. In the previous study, we found that the energy spectrum distortion at the junction of pig stomach tissue and pork tissue was different from that of these two tissues, and based on this finding, we proposed the conjecture of "biojunction". In order to study the reproducibility of this electrical feature, we use a variety of pig tissues to construct a new composite biological tissue for testing, and the results show that the feature can be reproduced in the artificially constructed composite biological tissue. Meanwhile, in order to study whether this electrical feature will appear at the boundary of naturally formed composite biological tissues and cancer tissues surrounded by normal tissues, we construct a tumor bearing mouse model carrying human ovarian cancer cells and tested it in the active electric field. The results show that this feature also appeared in the in-vivo experiment. Finally, in order to test the availability of the electrical characteristics of the junction of composite biological tissues, the KNN algorithm is used to train and classify the data collected in the experiment of tumor bearing mice, and the junction site and non-junction site of organic tissues are distinguished with a high success rate, showing the potential of this electrical characteristic in detecting the boundary of tumor tissues in clinic.

KEYWORDS

Active electric field, Composite biological tissue, Electrical characteristics, Tumor bearing mouse model.

INTRODUCTION

Cancer is a highly dangerous disease characterized by the uncontrolled growth and invasion of malignant cells into surrounding tissues, with a tendency to metastasize throughout the body. Current common treatment methods for cancer include surgery, chemotherapy, radiotherapy, targeted therapy, and immunotherapy [1]. In the surgical treatment of cancer, ensuring the precise and complete removal of cancerous tissue while maximizing the preservation of normal tissue around the lesion can reduce surgical damage to the patient's healthy organs and significantly improve the success rate of the surgery [2,3].

Therefore, accurately identifying the boundaries of cancerous tissue is an extremely important aspect of tumor surgery.

Traditional imaging techniques such as CT and MRI can only provide an approximate location of tumors before surgery and are unable to offer real-time images during the surgical process. Imaging technologies like ultrasound, due to the obstruction by organs and surgical instruments, struggle to produce high-quality images [4]. Particularly in the case of ovarian cancer, which typically occurs within the patient's abdominal cavity, this harsh environment poses significant challenges for imaging technologies and boundary identification techniques. Moreover, malignant

This is an open access article licensed under the Creative Commons Attribution 4.0 International License, which allows for use, distribution, and reproduction in any medium as long as the original work is properly cited. The Authors © 2025. The International Association of Advanced Materials, Sweden, publishes Advanced Materials

Advanced Materials Letters

https://aml.iaamonline.org



ovarian cancer often extends beyond the ovaries, with cancerous tissues potentially spreading through the peritoneal fluid to other abdominal organs, such as the fallopian tubes and uterus. This widespread and complex distribution greatly complicates the accurate identification of tumor boundaries during surgery [5,6].

To address these challenges in identifying tumor boundaries during surgery, we propose a new method based on the principle of biomimetic active electric fields to assist in detecting the boundaries of tumor tissues surrounded by normal tissue in tumor surgery. This new method draws inspiration from the natural behavior of weakly electric fish, which use electric fields for activities such as evading predators, hunting, and navigation in complete darkness by emitting electric fields and perceiving disturbances in the field caused by objects [7-10]. In the application of the biomimetic active electric field principle, this technology has demonstrated potential in identifying different shapes and materials of inorganic metals [11,12]. This achievement inspired us to apply biomimetic active electric field technology to the identification of boundaries between organic tissues, particularly between tumor surrounding normal tissues.

In previous experiments, we observed that when active electric field detection was applied to artificially constructed composite biological tissues, a distinct electrical frequency response occurred at the boundary between pork stomach tissue and pork tissue, differing from the responses of the two homogeneous organic tissues. Utilizing this phenomenon, we could accurately calculate the size of heterogeneous tissues within the composite biological tissues, leading us to propose the "biological junction" hypothesis, which suggests that a unique electrical field response will occur at the interface of two organic tissues with different electrical properties [13]. To investigate the repeatability of this phenomenon in composite biological tissues composed of other organic tissue materials, we construct composite tissues from pig kidney, liver, and stomach tissues and observe the same special electrical characteristics at the boundaries of the different tissues. Based on this finding, we further hypothesize that in naturally formed composite biological tissues, such as cancerous tissues surrounded by normal tissue, this special electrical feature might also appear at the interface of the two tissues. To test this hypothesis, we construct a tumor-bearing mouse model with human ovarian cancer cells and conducted tests. We find that at the cancer-normal tissue boundary, there is a mutation in the characteristic amplitude value, indicating the presence of this special electrical property at the interface of organic tissues, which aligns with our previously proposed "biojunction" hypothesis.

From this perspective, if we can detect this electrical feature in real-time during surgery, i.e., the change in electrical characteristics at the junction of different organic tissues, it would greatly enhance the detection capability of tumor boundaries during surgery. This discovery provides

data support for integrating active electric field technology into surgical instruments, such as scalpels or endoscopic devices. Such integration would enable surgical instruments to provide real-time feedback on changes in electrical properties when encountering different types of tissues and tissue boundaries, thereby assisting doctors in making more precise judgments during surgery.

EXPERIMENTAL

On the basis of the previous experiments, we know that the measured frequency responses of the five organic tissues are different under electric fields of different frequencies, and on this basis, by constructing a composite bio-tissue and probing it, we obtain the conclusion that the electric field response at the junction of pork tissue and pork belly tissue is different from that of these two homogeneous organic tissues. This phenomenon is similar to the phenomenon of "PN junction" in physics, so we propose the conjecture of "biojunction" with reference to the "PN junction", i.e., when two organic tissues with different electric field responses come into contact with each other, the electric field response at the junction is different from that of the two materials [13].

In this study, we first refine the electric field frequency and attempt to construct composite biological tissues using other organic tissue materials in pairs. We have scanned the constructed composite biological tissues and tested the repeatability of the special electrical characteristics at the junction of the composite biological tissues. Subsequently, in order to explore the manifestation of this electrical characteristic in living tissues, we have conducted tests on tumor bearing mice carrying human ovarian cancer cells. We have chosen thymus free nude mice as the receptor. Considering the convenience of subsequent measurements, we have implanted human ovarian cancer cells into the legs of thymus free nude mice and redesigned the sensor module of the experimental device. Using this experimental setup, we have selected three points from the tumor center, tumor boundary, and normal tissue on the leg of the tumor bearing mouse species, and measured them under different frequency electric fields.

Experimental Device

In order to achieve the detection of organic tissues and their boundaries using biomimetic active electric field principles, we have built an active electric field detection experimental device by simulating the detection excitation of weak electric fish. Fig. 1 shows the overall overview of the experimental setup we built, which is mainly divided into the following four modules: (1) Sensor module, used to construct the electric field and collect signals; (2) Signal generation module, used to generate stable voltage signals and transmit them to the sensor module to construct an electric field; (3) The signal acquisition module is responsible for receiving the electric field distortion data collected by the sensor module and storing it for subsequent

OPEN ACCESS

processing; (4) The motion scanning module is used in onedimensional dynamic detection experiments to drive the sensor module to move and scan organic tissues.

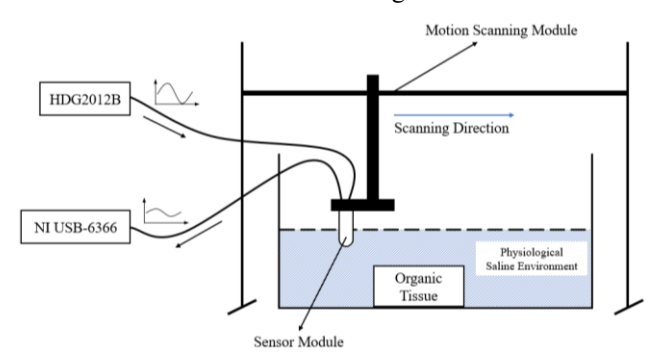


Fig. 1. Overall schematic diagram of the experimental setup.

For the sensor module, the sensor probe requires a pair of transmitting electrodes and receiving electrodes to construct the electric field and collect signals. Since the liquid environment selected for the experiment is saline, we choose platinum as the material for the electrodes, considering the stability, corrosion resistance, and repeatability of the electrode materials, and integrating the economic factors and the difficulty of obtainability. In order to make the electrodes collect more information in a smaller scale, the electrodes are made as circular platinum sheets and we position four electrodes on one sensor probe. In the tumor mouse experiment, in order to measure the tumor tissues of the mice, which are smaller in size compared to the organic tissues in the experiment, we redesign the sensor module to reduce the size of the electrodes and fixed the sensor module using a three-axis high-precision displacement stage, so that the sensor probes can be accurately aligned to the positions to be measured in the experiments. Fig. 2 shows the physical diagram of the sensor probe used in the experiment.

For the signal transmission module, we choose Hante's HDG2012B arbitrary waveform generator as the signal generator. In the experiment, the signal generator is directly connected to the transmitting electrode, and an underwater detection electric field is established through the generated signal.

For the signal acquisition module, we choose NI's USB-6366 data acquisition card as the device for collecting and receiving electrode signals, and use NI's matching acquisition program LabVIEW Signal Express to complete the functional configuration and driver control of USB-6366.

The scanning module mainly imitates the movement of weak electric fish in aquatic environments. In the process of detecting organic tissues, it is necessary to continuously move the sensor probe on the surface of the object to obtain organic tissue detection information. In this experiment, we use a three-axis stepper motor to drive the movement of a detection platform equipped with a sensor probe in a water tank. Fig. 3 shows a schematic diagram of the sensor probe scanning organic tissue.

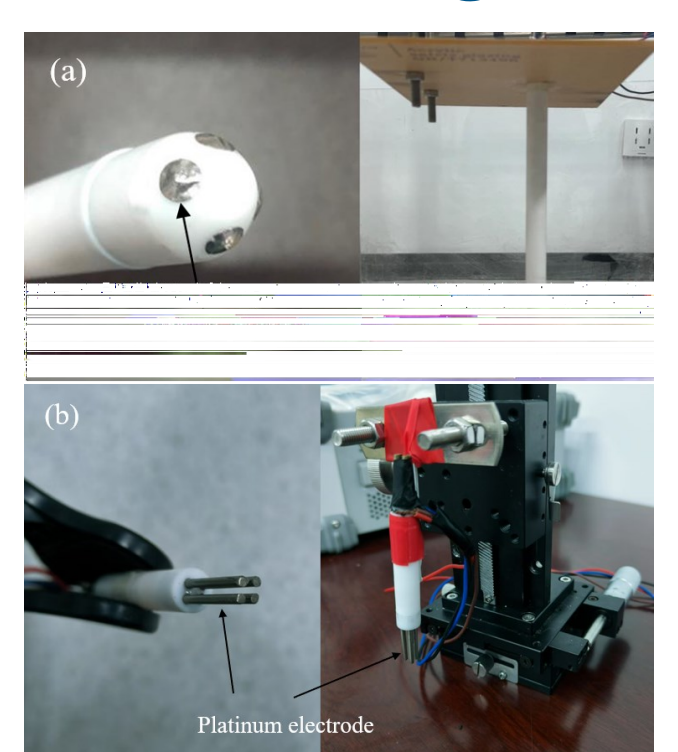


Fig. 2. Physical image of sensor probe: (a) Sensor probe used in one-dimensional dynamic detection experiment (b) Sensor probe used in single point experiment on tumor bearing mice.

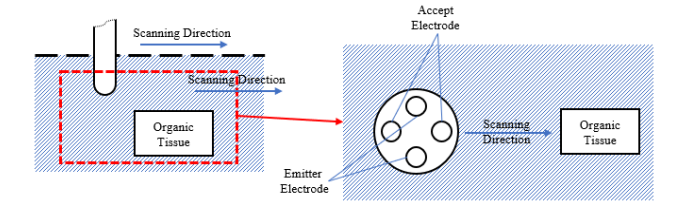


Fig. 3. Schematic diagram of scanning process.

Experimental Procedure

Our experiment is divided into two parts, one-dimensional dynamic detection experiment and single point detection experiment on tumor bearing mice. In the one-dimensional dynamic detection experiment, we use pig kidney tissue, pig liver tissue and pig stomach tissue to construct composite biological tissue, and refined the emitted electric field frequency to verify the repeatability of the "biojunction" phenomenon found in the previous experiment. In the single point detection experiment of tumor bearing mice, we sample the tumor growth sites of live tumor bearing mice at three points, namely the tumor center, tumor boundary, and normal tissue, and detected their electric field responses under different frequency electric fields. In both one-dimensional dynamic detection experiments and single point experiments on tumor bearing mice, a single frequency sine wave signal is selected as the electric field excitation signal. Details regarding the use of organic tissue materials and composite biomaterials will be explained in detail in the corresponding results section.



Experimental steps for one-dimensional dynamic detection:

- 1. Place organic tissue materials, adjust the material position, and ensure that the probe can pass through the center of the material during the scanning process.
- 2. Using a signal generator to emit sine wave signals of a specific frequency to establish an active electric field detection environment.
- 3. Control the movement of three-axis stepper motors in scanning modules equipped with sensor probes.
- 4. Using LabVIEW Signal Express to control USB-6366 to collect detection data during scanning process.
- 5. Conduct multiple repeated experiments and data collection for each frequency experimental group.
- 6. Conduct multiple experiments by changing the frequency of the transmitted signal.
- 7. Replace organic tissue materials or composite biomaterials, clean the experimental platform, and repeat steps 1-6.

Single point experimental procedure for tumor bearing mice:

- 1. Place tumor bearing mice in a constant temperature water bath, and adjust the position of tumor bearing mice for detection.
- Using a signal generator to emit sine wave signals of a specific frequency to establish an active electric field detection environment.
- 3. Aim the sensor probe at the selected point on the tumor site of the tumor bearing mouse.
- 4. Using LabVIEW Signal Express to Control USB-6366 for Data Acquisition.
- 5. Conduct multiple experiments by changing the frequency of the transmitted signal.
- 6. Change the detection point of the sensor probe or replace the experimental tumor bearing mouse, repeat steps 1-5.

RESULTS AND DISCUSSION

One Dimensional Dynamic Detection Experiment

Through preliminary experiments, it can be concluded that the electrical properties exhibited by pig stomach tissue during static detection are more stable compared to other tissues [13]. So, in this experiment, we choose pig stomach tissue as the material to simulate normal tissue, and select pig kidney tissue and pig liver tissue embedded in pig stomach tissue as the material to simulate cancer tissue. In both experiments, the size of pig stomach tissue used is 41.5mm, the size of pig liver tissue used is 28.8mm, and the size of pig kidney tissue used is 22.1mm. In the experiment, the constructed composite biological tissues are placed in a physiological saline environment with a conductivity of 4.56mS/cm and a temperature of 25 °C, and the composite biological tissues are scanned using a scanning module. During the scanning process, the scanning module is equipped with a sensor module that moves in a straight line at a speed of 10mm/s for 10 seconds. In the experiment, we use a signal generator to emit a sine wave signal with a frequency of 100Hz-1000Hz and an amplitude of 4V to establish an active electric field, with a frequency difference of 100Hz between the two signals.

For the data received by the sensor module, we use Short Time Fourier Transform (STFT) to process it and extract the energy distribution at different frequencies and time points in the signal. For the scanning data processing and visualization of pig stomach tissue, we can obtain a three-dimensional time-frequency joint graph at each frequency and energy slices of the time energy spectrum plane obtained along the frequency axis. By differentiating the energy slices, we can obtain the time point with the highest degree of distortion in the time energy spectrum. By combining this time point with the motion speed of the scanning module, we can obtain the size of the tissue to be tested. Fig. 4 shows the scan results obtained by simulating cancer tissue using pig kidney tissue and pig liver tissue, respectively. Here, we only present the results at an electric field frequency of 400Hz.

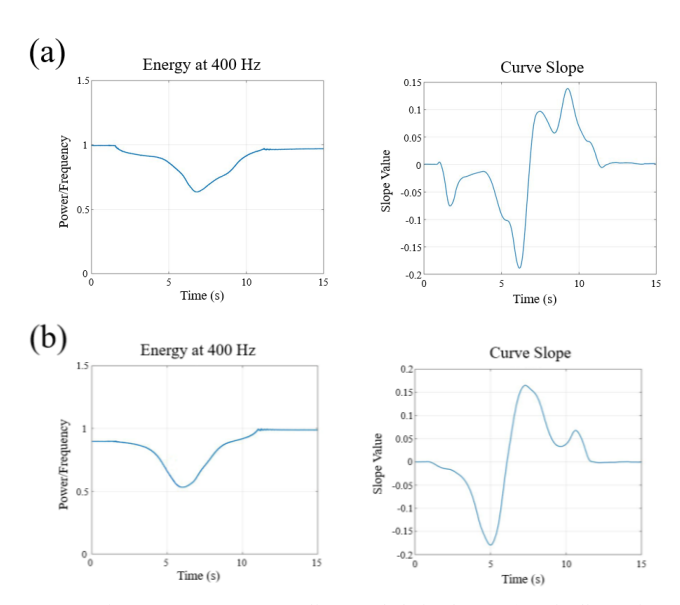


Fig. 4. Time energy spectrum slices and their slopes: (a) Pig liver pig stomach composite biological tissue (b) Pig kidney pig stomach composite biological tissue.

In our previous study [13], we observed significant electric field distortion at the boundaries of tissues due to substantial changes in electrical properties. This distortion may arise from the differences in polarization characteristics between distinct tissues, particularly when the electrode traverses the interface between two tissues with different electrical properties. This effect is manifested in the changes of the slope of the energy slices, and it has successfully been utilized to calculate the dimensions of the pork tissue, acting as a heterogeneous medium, by identifying the time points at which the extrema of the slope occur, using pork-bowel composite biological tissues as the subject for detection experiments.



In the present study, we continued the approach developed in our previous research for the calculation of the size of heterogeneous tissues within composite biological tissues. Based on the time points of the maximum and minimum slope values in the graph, combined with the motion speed of the scanning module, it can be concluded that under an electric field of 400Hz, the calculated size of pig kidney tissue is 23.7mm, and the calculated size of pig liver tissue is 29.8mm. By repeating this data processing process, we can obtain the calculated values of pig liver tissue size and pig kidney tissue size under various frequency electric fields, as shown in **Table 1**.

Table 1. Calculated Composite Biological Tissue Size and Error.

| Frequency | Pig liver tissue size | Size error of pig liver tissue | Pig kidney tissue size | Size error of pig kidney tissue |
|-----------|--------------------------|--------------------------------------|---------------------------|---------------------------------------|
| 100 Hz | 30.9mm | 7.29% | 23.2mm | 4.97% |
| 200 Hz | 29.9mm | 3.82% | 22.8mm | 3.17% |
| 300 Hz | 30.5mm | 5.90% | 23.5mm | 6.33% |
| 400 Hz | 29.8mm | 3.47% | 23.7mm | 7.24% |
| 500 Hz | 29.5mm | 2.43% | 22.7mm | 2.71% |
| 600 Hz | 30.6mm | 6.25% | 21.9mm | -0.90% |
| 700 Hz | 30.8mm | 6.94% | 39.4mm | 78% |
| 800 Hz | 30.3mm | 5.21% | 21.4mm | -3.17% |
| 900 Hz | 30.2mm | 4.86% | 21.7mm | -1.81% |
| 1000Hz | 30.9mm | 7.29% | 20.4mm | -7.69% |

In this set of data, there is an abnormal data in the detection and calculation of pig kidney tissue in an electric field with a frequency of 700Hz, resulting in a large error. In response to this, we hypothesize that the combined influence of polarization effects in electric fields of different frequencies and the electrochemical properties of tissues results in an intersection of the electrical characteristics exhibited by the pork belly tissue, acting as normal tissue, and the pork kidney tissue, acting as the heterogeneous tissue, when the electric field frequency approaches approximately 700 Hz. The difference in electrical characteristics between the two tissue types is less than the difference between the pork belly tissue and the surrounding aqueous environment. Consequently, the change in electrical characteristics at the interface between the two tissues is smaller than the slope of the change in electrical characteristics at the interface between the pork belly tissue and the aqueous environment. This would lead to misidentification of the pork belly tissue dimensions as those of the pork kidney tissue when using the aforementioned calculation method. The geometric size determined, 39.4 mm, is also significantly closer to the size of the pork belly tissue, which is 41.5 mm.

After excluding the outlier, the data analysis in the table shows that using the time point with the highest degree of distortion in the time energy spectrum as the sensor module to scan the time point passing through the junction of composite biological tissues, and combining the scanning speed to obtain the size of heterogeneous tissues embedded in pig stomach tissue, can relatively accurately

obtain the size of heterogeneous tissues. This conclusion demonstrates the feasibility of using the maximum degree of distortion in the time energy spectrum to determine the junction of composite biological tissues, as well as the reproducibility of pre-experimental and special electrical characteristics at artificially constructed composite biological tissue junction.

Single Point Experiment on Tumor Bearing Mice

In order to investigate whether there are special electrical characteristics at the junction of non-artificially constructed composite biological tissues, namely naturally formed cancer tissues surrounded by normal tissues, we conduct a probe on a tumor bearing mouse model carrying human ovarian cancer cells. To test the reproducibility of the experiment, we construct 5 tumor bearing mouse models.





Fig. 5. Schematic diagram of tumor bearing mouse experiment: (a) Schematic diagram of collection points at the cancer center, normal tissue, and cancer tissue normal tissue junction of tumor bearing mice (b) Schematic diagram of data collection process

When constructing the tumor bearing mouse model, considering the convenience of collecting data in the experiment, we transplant human ovarian cancer cells into the legs of thymus free nude mice and allowed them to grow naturally. When collecting the data, we select three points for detection: the center of tumor tissue observed, the junction between tumor tissue and normal tissue by the naked eye, and normal tissue, as shown in **Fig. 5.** During the detection process, in order to prevent the deviation of data collection points caused by the movement of tumor



bearing mice, we anesthetize them with Tribromoethanol Afudine. And to prevent the tumor bearing mice from losing temperature during the experiment, we place them in a constant temperature physiological saline water bath at 34 degrees Celsius for detection. The conductivity of physiological saline is 4.56mS/cm. In the experiment, we use a signal generator to emit a sine wave signal with a frequency of 100Hz-1500Hz and an amplitude of 4V to establish an active electric field, with a frequency step of 100Hz between the two signals.

We use Fast Fourier Transform (FFT) to process the data received by the sensor module, in order to extract the amplitude corresponding to the frequency of the emitted electric field during each experiment. **Table 2** shows the results of collecting two tumor bearing mice after natural growth for 35 days after tumor cell implantation. **Fig. 6** visualizes the data in the form of amplitude-frequency curves.

Table 2. Amplitude frequency response data of different parts of tumor bearing mice (V).

| | Tumor Bearing Mice 1 | | | Tumor Bearing Mice 2 | | |
|-----------|---------------------------------|---------------|------------------|---------------------------------|---------------|------------------|
| Frequency | Center of Tumor Tissue | Bounda- ry | Normal Tissue | Center of Tumor Tissue | Bounda- ry | Normal Tissue |
| 100Hz | 0.0483 | 0.0610 | 0.0595 | 0.0352 | 0.0325 | 0.0442 |
| 200Hz | 0.0825 | 0.1045 | 0.0958 | 0.0633 | 0.0685 | 0.0964 |
| 300Hz | 0.1075 | 0.1371 | 0.1245 | 0.0930 | 0.0967 | 0.1347 |
| 400Hz | 0.1290 | 0.1646 | 0.1469 | 0.1171 | 0.1158 | 0.1707 |
| 500Hz | 0.1475 | 0.1879 | 0.1642 | 0.1374 | 0.1319 | 0.1975 |
| 600Hz | 0.1632 | 0.2079 | 0.1788 | 0.1531 | 0.1452 | 0.2194 |
| 700Hz | 0.1765 | 0.2243 | 0.1904 | 0.1676 | 0.1566 | 0.2360 |
| 800Hz | 0.1876 | 0.2384 | 0.1998 | 0.1774 | 0.1654 | 0.2486 |
| 900Hz | 0.1968 | 0.2499 | 0.2075 | 0.1850 | 0.1725 | 0.2579 |
| 1000Hz | 0.2042 | 0.2597 | 0.2133 | 0.1909 | 0.1756 | 0.2660 |
| 1100Hz | 0.2103 | 0.2671 | 0.2177 | 0.1950 | 0.1782 | 0.2730 |
| 1200Hz | 0.2151 | 0.2727 | 0.2207 | 0.1978 | 0.1807 | 0.2750 |
| 1300Hz | 0.2187 | 0.2776 | 0.2228 | 0.2001 | 0.1783 | 0.2766 |
| 1400Hz | 0.2214 | 0.2804 | 0.2236 | 0.2005 | 0.1790 | 0.2791 |
| 1500Hz | 0.2231 | 0.2823 | 0.2239 | 0.1982 | 0.1777 | 0.2716 |

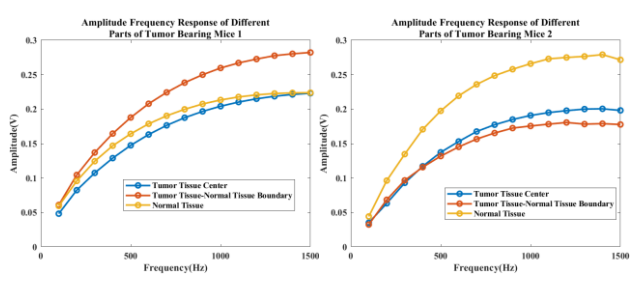


Fig. 6. Amplitude-frequency response of different parts of tumor bearing mice.

In order to more intuitively observe the amplitude frequency response relationship between the three parts of tumor bearing mice at various frequencies, we slice and visualize the amplitude-frequency response of each frequency point. **Fig. 7** shows the amplitude frequency response relationship of the three parts of two tumor bearing mice at frequencies of 100Hz, 500Hz, 900Hz, and 1300Hz.

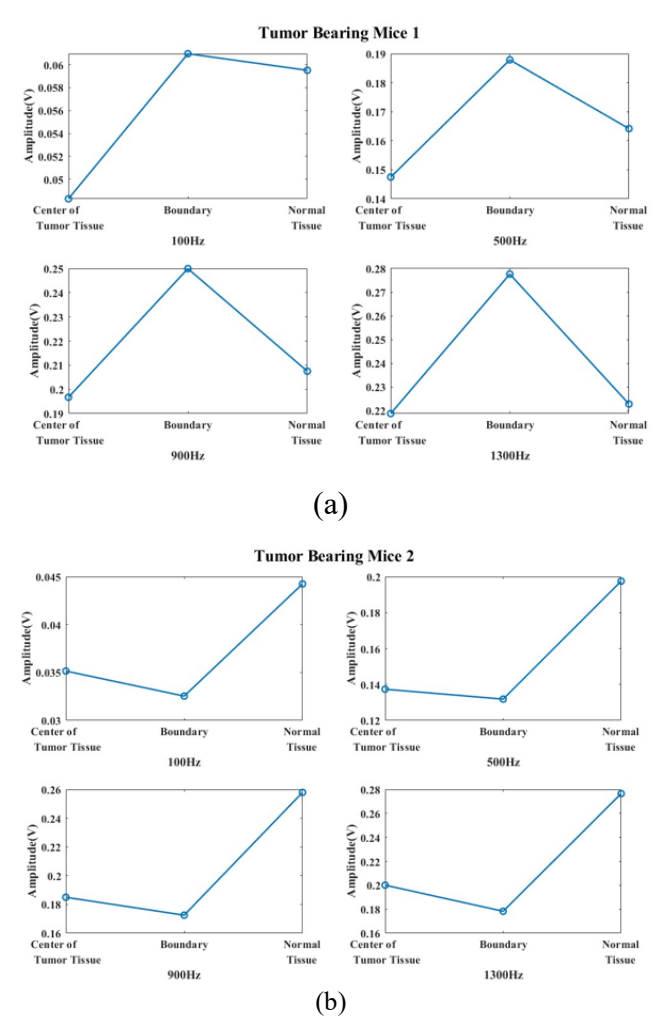


Fig. 7. Amplitude frequency response relationship of three parts of tumor bearing mice at different frequencies: (a) Tumor bearing mice 1; (b) Tumor bearing mice 2.

From Fig. 7, it can be seen that although the amplitude frequency curves of the three parts of these two tumor bearing mice are not completely the same on the vertical axis, the amplitude frequency curves at the cancer tissue normal tissue junction, the cancer tissue center, and the normal tissue are significantly different. Compared with the mutation of these two tissues, based on this finding, we collect data from the cancer-to-normal tissue junction of five tumor bearing mice and recorded the probability of their amplitude frequency response appearing at the maximum of the three parts and between normal tissue and cancer tissue. The results are shown in Table 3.

OPEN ACCESS

Table 3. Location and probability of amplitude frequency response at the junction of cancer tissue and normal tissue.

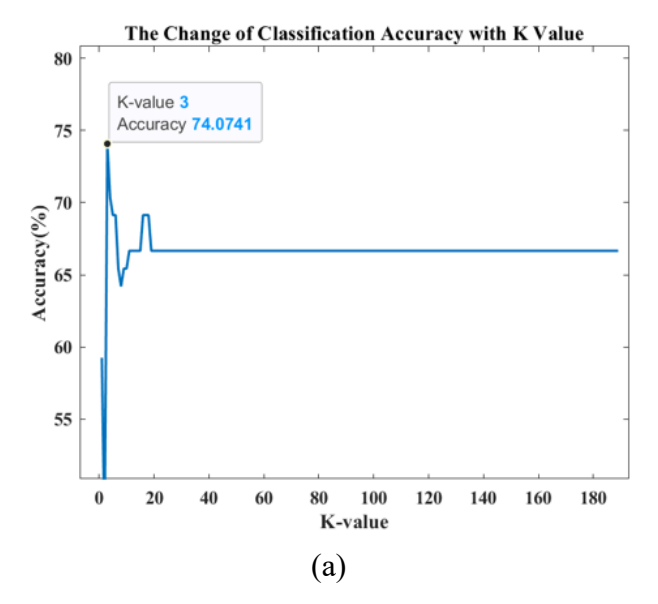
| Appearance Location | At the Maximum or Minimum Amplitude Frequency Response Value | Between the Amplitude Frequency Response of Cancer Tissue and Normal Tissue |
|------------------------|-----------------------------------------------------------------------|--------------------------------------------------------------------------------------|
| Probability | 73.3% | 26.7% |

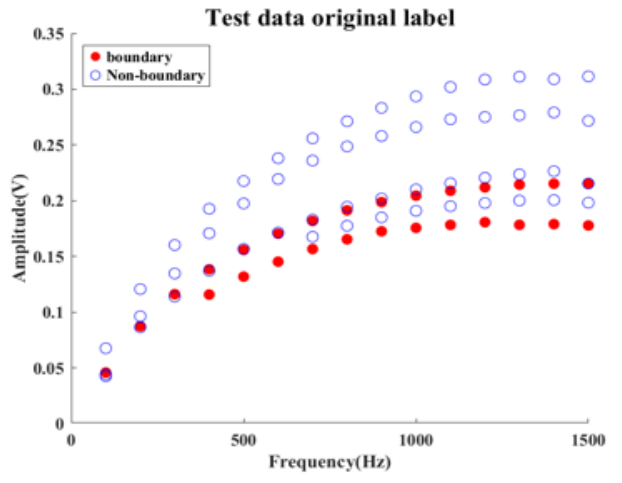
According to the statistical results, when detecting the cancer tissue center, normal tissue, and cancer tissue normal tissue junction of tumor bearing mice, 73.3% of the amplitude-frequency response at the cancer-to-normal tissue junction appear at the peak of the three locations, which is the same as the point with the highest degree of temporal energy spectrum distortion at the composite biological tissue junction in one-dimensional dynamic detection experiments, compared to the occurrence of mutations in cancer tissue and normal tissue. This conclusion indicates that the special electrical characteristics at the junction of composite biological tissues have also been observed in in in vivo experiments. Based on this discovery, we further propose a hypothesis: by discovering this feature, can we distinguish between the boundaries and non-boundaries of different tissues?

In order to demonstrate that the special electrical characteristics of composite biological tissue junctions in living organisms can be used to distinguish between different tissue junctions and tissue centers, we use the K-Nearest Neighbor (KNN) algorithm to classify them. The steps for training and classification by the KNN algorithm are [14]:

- 1. Normalize the data that needs to be classified
- 2. Given a test set sample, calculate its distance from each of the training set samples;
- The K training set samples that are closest to the test set samples are selected as the nearest neighbours of the test set samples;
- 4. Decide the labels of the test set samples based on the labels to which most of the samples in these K nearest neighbours belong.

During this process, we select 5 tumor bearing mice and classified the data collected at 25 and 35 days of natural growth after tumor implantation. We first normalize the data by subtracting the mean value, and pre-divide the data into two categories: tissue boundary and non-boundary based on whether it is at the junction of cancer tissue and normal tissue. Then we randomly select 315 sets of data (70%) as the training set for the classified samples, and the remaining 135 sets of data (30%) as the test set for classification. During the training process, frequency and characteristic amplitude manifested as special electrical features are used as classification features to classify whether it is a tissue junction. The classification results of the KNN algorithm vary with different values of K, as shown in Fig. 8. When K reaches 3, the classification accuracy is the highest, at 74%.





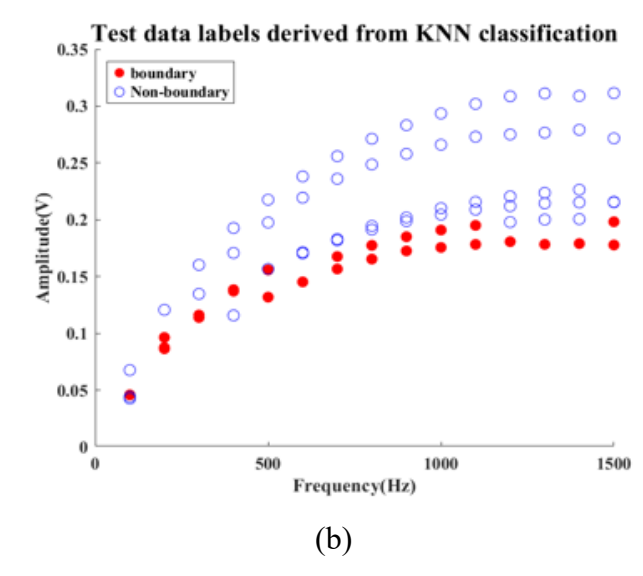


Fig. 8. Classification results of KNN algorithm: (a) Changes in classification accuracy with K value (b) Comparison of original labels and classified labels in test data when K=3.

Advanced Materials Letters

https://aml.iaamonline.org



In this section, we use KNN to classify the amplitude frequency response at three locations of tumor bearing mice that exhibit special electrical characteristics. From the classification results of KNN, it can be seen that although there are some errors, using the characteristic amplitude frequency response manifested as special electrical features combined with KNN algorithm can still accurately determine whether the measured position is at the tissue boundary.

CONCLUSION

Based on the previous experiments and studies, we obtained the conclusion that the electric field response at the junction of two kinds of tissues in the composite biological tissue composed of pork tissue and pig stomach tissue is different from the two kinds of homogeneous organic tissues, and put forward the "biojunction" conjecture.

In this study, we construct a new composite biological tissue by combining pig stomach tissue, pig kidney tissue, and pig liver tissue in pairs to explore the repeatability of this special electrical characteristic at the junction of other organic tissue materials. We conduct active electric field scanning experiments on new composite biological tissues. By combining the point with the highest degree of temporal energy spectrum distortion and scanning speed, we are able to calculate the size of heterogeneous tissues in composite biological tissues with minimal error. This conclusion demonstrates the feasibility of using the point with the highest degree of temporal energy spectrum distortion to determine the junction of composite biological tissues, as well as the repeatability of the previous experiments and the special electrical characteristics of artificially constructed composite biological tissue junctions.

Subsequently, in order to investigate whether there would be similar electrical characteristics at the junction of non-artificially constructed composite biological tissues, namely naturally formed cancer tissues surrounded by normal tissues, we construct a tumor bearing mouse model and collected data from three points on the model: the cancer tissue center, normal tissues, and the cancer-tonormal tissue junction. Through the analysis of the collected data, we have found that the data at the cancer normal tissue junction showed mutation compared with the other two points. According to the statistics of the data, we have found that 73.3% of the amplitude frequency response at the cancer normal tissue junction should fall at the maximum value of the amplitude frequency response of the three parts, which is the same as the special electrical characteristics found in the test of artificial composite biological tissue, in line with our biojunction conjecture. Furthermore, to investigate whether this feature can be used to distinguish between tissue boundaries and tissue centers, we have trained and classified the collected data using the KNN algorithm. The KNN algorithm is able to distinguish whether it is a tissue boundary with 74% accuracy. Despite the existence of errors, the use of characteristic amplitude frequency responses manifested as special electrical features at the junction of composite biological tissues combined with KNN algorithm can still accurately determine whether the measured location is at the tissue junction.

Although the cancer tissue boundaries identified through this method have a certain misjudgment rate due to differences in tumor growth in tumor bearing mice, its noninvasive, easy to operate, and cost-effective advantages make it a powerful tool for evaluating organic tissue size. Future research should further explore how to improve the accuracy of judgment by adjusting frequency and adopting advanced signal processing techniques, and optimize electrode design for integration with surgical knives, endoscopes, and other equipment. In this study, the biojunction conjecture is only in the stage of phenomenon recognition and preliminary verification, and its principle is not analyzed. However, it can be predicted that a deep understanding of this special electrical feature will provide a new perspective for disease diagnosis, especially in identifying and locating tumor boundaries.

In future research, we will explore how to optimize the accuracy of distinguishing cancer tissue normal tissue boundaries by utilizing the special electrical characteristics of composite biological tissue boundaries, in order to improve their application efficiency in biomedical imaging and treatment, and open up new directions for the fields of bioelectronics and medical imaging.

ACKNOWLEDGEMENTS

This work was supported by Natural Science Foundation of Sichuan Province (2022NSFSC0800) and National Natural Science Foundation of China (62273075).

CONFLICTS OF INTEREST

There are no conflicts to declare.

REFERENCES

- Wang, S.; Liu, Y.; Feng, Y.; Zhang, J.; Swinnen, J.; Li, Y.; Ni, Y; Cancers, 2019, 11 (11), 1782.
- Song, S. S.; Goldenberg, A.; Ortiz, A.; Eimpunth, S.; Oganesyan, G.; Jiang, S. I. B.; JAMA Dermatol., 2016, 152 (6), 683-690.
- 3. Lei, K. F.; Micromachines, **2014**, 5 (1), 1-12.
- Xu, J.; Tan, Y.; Zhang, M.; Zhejiang Daxue Xuebao, Yixueban, 2017, 46 (5), 455-461.
- Nougaret, S.; Sadowski, E.; Lakhman, Y.; Rousset, P.; Lahaye, M.; Worley, M.; Sgarbura, O.; Shinagare, A. B.; DIAGN INTERV IMAG, 2022, 103 (10), 448-459.
- Mei, S.; Chen, X.; Wang, K.; Chen, Y.; Cancer Cell Int., 2023, 23 (1), 11.
- Nelson, M. E.; MacIver, M.; J. Comp. Physiol., A, 2006, 192 (6), 573-586.
- 8. Avril, A.; Graff, C.; J. Comp. Physiol., A, 2007, 193 (12), 1221-1234.
- 9. Lissmann, H. W.; Machin, K. E.; J. Exp. Biol., 1958, 35 (2), 451-
- 10. von der Emde, G.; J. Comp. Physiol., A, **2006**, 192 (6), 601-612.
- Caputi, A. A.; Budelli, R.; Grant, K.; Bell, C. C.; J. Exp. Biol., 1998, 201 (14), 2115-2128.
- 12. Peng, J.; Bioinspiration Biomimetics, 2015, 10 (6), 066007.
- Wang, L.; Tian, T.; Yang, W.; Yang, C.; Peng, J. Organic heterogeneous tissue boundary detection based on the principle of

Advanced Materials Letters

https://aml.iaamonline.org



- active electric field. Academic Conference of China Instrument and Control Society, 2024, 777-783.
- 14. Uddin, S.; Haque, I.; Lu, H.; Moni, M. A.; Gide, E.; Sci. Rep., **2022**, 12 (1), 6256.

AUTHORS BIOGRAPHY

Cong Yang, Long Wang, and Dehao Yin are currently pursuing a Master's degree in School of Automation Engineering at the University of Electronic Science and Technology of China, focusing on researching new sensors based on active electric fields.

Dr. Tian Tian is the attending physician of the Obstetrics and Gynecology Department of Sichuan Provincial People's Hospital. She has professional advantages in prenatal diagnosis, etiological examination and treatment of recurrent miscarriages, as well as genetic diagnosis of congenital reproductive system abnormalities.

Pro. Jiegang Peng, from the University of Electronic Science and Technology of China, specializes in sensor technology and robotics. With a Ph.D. from Zhejiang University and postdoctoral research at Tsinghua University, he has led national projects, authored "Principles and Applications of Sensors," and published over 30 papers. He's a Fellow of the International Association of Advanced Materials for his work in biosensors, bioelectronics, and biodevices.





This article is licensed under a Creative Commons Attribution 4.0 International License, which allows for use, sharing, adaptation, distribution, and reproduction in any medium or format, as long as appropriate credit is given to the original author(s) and the source, a link to the Creative Commons license is provided, and changes are indicated. Unless otherwise indicated in a credit line to the materials, the images or other third-party materials in this article are included in the article's Creative Commons license. If the materials are not covered by the Creative Commons license and your intended use is not permitted by statutory regulation or exceeds the permitted use, you must seek permission from the copyright holder directly.

Visit http://creativecommons.org/licenses/by/4.0/ to view a copy of this license